



HAL
open science

The pink staircase of Sully-sur-Loire castle: Even bacteria like historic stonework

Johann Leplat, Faisl Boustia, Alexandre François, Mikael Guiavarc'H, Jean-Didier Mertz, Didier Brissaud

► To cite this version:

Johann Leplat, Faisl Boustia, Alexandre François, Mikael Guiavarc'H, Jean-Didier Mertz, et al.. The pink staircase of Sully-sur-Loire castle: Even bacteria like historic stonework. *International Biodeterioration and Biodegradation*, 2019, 145, 10.1016/j.ibiod.2019.104805 . hal-02470673

HAL Id: hal-02470673

<https://univ-rennes.hal.science/hal-02470673>

Submitted on 20 Jul 2022

HAL is a multi-disciplinary open access archive for the deposit and dissemination of scientific research documents, whether they are published or not. The documents may come from teaching and research institutions in France or abroad, or from public or private research centers.

L'archive ouverte pluridisciplinaire **HAL**, est destinée au dépôt et à la diffusion de documents scientifiques de niveau recherche, publiés ou non, émanant des établissements d'enseignement et de recherche français ou étrangers, des laboratoires publics ou privés.



Distributed under a Creative Commons Attribution - NonCommercial 4.0 International License

1 **The pink staircase of Sully-sur-Loire castle: even bacteria like historic**
2 **stonework.**

3
4
5

6 Johann Leplat^{ab*}, Faisl Bousta^{ab}, Alexandre François^{ab}, Mikaël Guiavarc'h^{ab1}, Jean-Didier
7 Mertz^{ab}, Didier Brissaud^{ab}

8
9

10 ^a Laboratoire de Recherche des Monuments Historiques (LRMH), Ministère la Culture, 29 rue
11 de Paris, 77420 Champs-sur-Marne, France

12 ^b Sorbonne Universités, Centre de Recherche sur la Conservation (CRC, USR 3224), Museum
13 national d'Histoire naturelle, Ministère de la Culture et de la Communication, CNRS; CP21,
14 36 rue Geoffroy-Saint-Hilaire, 75005 Paris, France

15
16

17 * Corresponding author: johann.leplat@culture.gouv.fr

18 Laboratoire de Recherche des Monuments Historiques (LRMH), Ministère la Culture, 29 rue
19 de Paris, 77420 Champs-sur-Marne, France

20 Phone number: +33 1 60 37 77 97

21
22
23
24
25
26
27
28
29
30
31
32
33
34
35

¹ Present address: Laboratoire Archéosciences, UMR 6566 CReAAH, Université de Rennes 1
- Campus de Beaulieu, 263 avenue du Général Leclerc, CS 74205, 35042 Rennes Cedex,
France

36 **Abstract**

37

38 Rosy discoloration has affected the stone steps in the main spiral staircase of the Sully-sur-
39 Loire castle donjon for many years now. This study monitors the development of the
40 coloration and the environmental climatic conditions in the staircase to understand the
41 conditions favoring the presence of this rosy discoloration. High-throughput sequencing was
42 performed on healthy stone and on pink pigmented stone to identify the agent responsible for
43 this discoloration. The results suggest that the rosy discoloration is the mark of a former
44 degradation process which is now inactive, and that bacteria were the main agent of the pink
45 patina formation. *Nitiliruptor* was the main genus identified in the pink parts of the staircase.
46 This is the first time that this bacterial genus has been linked to a cultural heritage
47 biodeterioration process. There was no evidence that this bacterial genus was responsible for
48 the development of the pink patina, but it could have replaced it as a subsequent evolution of
49 the process.

50

51 **Keywords**

52

53 Cultural heritage preservation, stone biodeterioration, rosy discoloration, high-throughput
54 sequencing, *Nitiliruptor* sp., climatic monitoring

55

56 **1. Introduction**

57

58 Stone is one of the main and oldest materials used for artistic expression in the field of
59 cultural heritage. It was already used during the upper Paleolithic (between 50 000 and 10 000
60 years ago) as a support for engraving and sculpting in shelters and caves (Abadía and
61 Morales, 2013). The use of stone ranges from monumental constructions to the sculpture of
62 small statues.

63 The different types of stone used in the field of cultural heritage include marble, limestone,
64 sandstone and granite, and even man-made stones such as brick, mortar or concrete. Whatever
65 the type of stone used, they are all subject to some degree of biodeterioration (Warscheid and
66 Braams, 2000). This process is defined as an undesirable change in the properties of material
67 caused by the activity of biological agents (Hueck, 1965). The intensity of the biodeterioration
68 process on stone monuments depends on the intrinsic properties that define the bioreceptivity
69 of each stone (Guillitte, 1995; Miller et al., 2012), combined with the effects of climatic
70 changes and air pollution (Brimblecombe and Grossi, 2009; Caneva et al., 1995; Thornbush
71 and Viles, 2006).

72 The detrimental effects of organisms on stone monuments may be aesthetic, chemical and/or
73 physical (Scheerer et al., 2009). For example, the secretion of inorganic and organic acids by
74 organisms on stones leads to a process known as biocorrosion. This results in the dissolution
75 of the mineral matrix of the stone and the precipitation of salts, possibly causing physical
76 stress in the stone (McNamara and Mitchell, 2005; Warscheid and Braams, 2000). Organisms
77 can also enter the stone via pores in the material, causing mechanical damage and changing
78 the physical properties of the structural material (Scheerer et al., 2009; Sterflinger and Piñar,
79 2013).

80 Different types of organisms can be involved in biodeterioration, with both macro and
81 microorganisms observed. Phototrophic microorganisms such as algae and cyanobacteria are
82 generally considered as the initial colonizers (pioneer organisms) and produce colored patinas
83 and incrustations on stone monuments (Crispim and Gaylarde, 2005; Macedo et al., 2009),
84 whilst lichens grow much more slowly (Hoppert and König, 2006). The presence of these first
85 colonizers facilitates colonization by chemo-organotrophic bacteria and fungi (Gorbushina et
86 al., 2005; Li et al., 2016), which are strongly involved in the physical and chemical
87 deterioration process of stone monuments (Pinheiro et al., 2018; Salvadori and Municchia,
88 2016). Some chemo-organotrophic organisms have also been found on stone monuments
89 without the presence of pioneer organisms, and use organic matter derived from rock mineral,
90 airborne particles or products used in preceding restorations (Scheerer et al., 2009; Warscheid
91 and Braams, 2000). Higher plants are macro-organisms, and may thus play a role in the
92 biodeterioration of stone monuments by an initial colonization of monuments by pioneer
93 plants (herbaceous annuals and perennials) that cause minor damage and are then replaced by
94 shrubs or trees, which can cause substantial physical damage (Korkanç and Savran, 2015;
95 Lisci et al., 2003).

96 Within the biodeterioration process, the phenomenon of rosy discoloration of stones and wall
97 paintings has attracted increasing amounts of interest over recent years (De Felice et al., 2010;
98 Eettenauer et al., 2014; Gurtner et al., 2000; Imperi et al., 2007; Laiz et al., 2009; Piñar et al.,
99 2014b; Tescari et al., 2018b). This type of discoloration has been described in subterranean
100 and non-subterranean environments and has been widely reported in central and southern
101 Europe (Piñar et al., 2014a). Actinobacteria belonging to *Rubrobacter* genus were found to be
102 involved in discoloration in most of these cases (Jurado et al., 2012; Laiz et al., 2009; Nugari
103 et al., 2009; Schabereiter-Gurtner et al., 2001). In some other cases, other pink pigmented
104 bacteria such as *Arthrobacter*, *Rhodococcus* or *Methylobacterium* were identified (Piñar et al.,
105 2014b; Tescari et al., 2018a; Tescari et al., 2018b). The common link between the different
106 monuments affected by the development of pink biofilms seems to be water infiltration (Piñar
107 et al., 2014a). The crystallization of salts that occurs with these infiltrations may offer optimal
108 growth conditions for halophilic microorganisms in addition to their own destructive effect on
109 the stone.

110 In France, rosy discolorations are observable in Sully-sur-Loire castle. It is far from being the
111 only monument affected by this phenomenon in France, but it is one of the first to have been
112 intensively studied (Berdoulay and Salvado, 2009). The castle is one of the monuments listed
113 by UNESCO in the Loire Valley in 2000. It is located in the far eastern sector of the area
114 listed by UNESCO in the Loiret region. There has been a castle at this location on the left
115 bank of the Loire since the 12th century, but the construction of the current castle began at the
116 end of the 14th century. Additions and transformations were carried out until the 19th century.
117 Large reconstructions occurred in the 20th century after a great fire in 1918 and damage from
118 bombings during World War II. The castle is made of white tufa, which was the stone
119 typically used as a building material in the Loire Valley during the Renaissance period. Tufa
120 is a yellowish-white, porous and very fine-grained siliceous limestone with a small amount of
121 clayey minerals (Janvier-Badosa et al., 2015). The geometrical and symmetrical distribution
122 of the rosy discoloration on the stones of Sully-sur-Loire castle made it a remarkable study
123 case to compare and determine the conditions affecting its development.

124 The aim of this study was to confirm or exclude a biological origin for rosy discoloration,
125 and, if applicable, identify the organisms responsible for the biofilm development. In a second
126 step, we sought to compare the environmental conditions in areas of stone affected by rosy
127 discoloration with those observed in healthy areas to widen our knowledge of the factors that
128 lead to this phenomenon.

129
130
131
132

133 **2. Materials and Methods**

134

135 *2.1 Study area*

136 The rosy discoloration has only been observed on indoor stones and mainly in the “escalier
137 d’honneur”: the main spiral staircase of the donjon (Fig.1a). Not all the steps are affected to
138 the same extent by pink coloration, which is mainly located between the first and the second
139 floor, on the underside of the steps and exclusively on the outer part of the steps (Fig. 1b). The
140 steps range from those with no pink coloration to those with almost 75 % of their surface
141 affected by pink coloration.

142 Two of the most severely affected steps between the first and the second floor were chosen
143 for this study. This area had the further advantage of being closed to the public. The first step
144 was used for colorimetric and climatic monitoring (Fig. 2), while the second was sampled for
145 metagenomic microbial analysis.

146

147 *2.2 Colorimetric monitoring*

148 Colorimetric monitoring was used to characterize the initial differences between the white
149 area (unaffected) and the pink area (affected) of a given stone step and then to monitor the
150 progression of the coloration within and between these two sections through time according to
151 different factors. The chosen step was first divided into two parts: white and pink
152 (Supplementary fig. 1). Four measurement sections were then delineated within each of these
153 two sections: *i*) section scratched with a scalpel to remove the outside layer of the stone then
154 covered to hide it from direct light; *ii*) section scratched but not covered; *iii*) section covered
155 but not scratched; *iv*) control section left unscratched and not covered. Scratching removed
156 the coloration in the pink section and would thus enable us to observe any return of this
157 coloration. Covering was carried out to check for a possible role of light in the development
158 of the pink coloration. The first colorimetric measurements were made in September 2014
159 before and after scratching, then colorimetric progression was regularly checked over a three-
160 year period: in May 2015, January 2016, July 2017 and January 2018.

161 The measurements were made in each defined section with a Chroma meter CR-410 (Konica
162 Minolta, Tokyo, Japan), which uses the L*a*b* CIE 1976 color space under D65 illuminant,
163 and 10° observer. Each measurement returns three values assessed on a sample with a 5 cm
164 diameter: the L* value for lightness (0=black, 100=white); the a* value for the green-red
165 component (-120=green, 120=red); and the b* value for the blue-yellow component (-
166 120=blue, 120=yellow). Each color value was obtained using the mean of two replicated
167 measurements.

168

169 *2.3 Raman spectroscopy*

170 Raman spectroscopy was used on the pink powder obtained after scratching the stone to
171 characterize the pigment involved. Analysis was performed using an InVia confocal Raman
172 microscope (Renishaw, Wotton-under-Edge, UK) equipped with a 785-nm laser diode and a

173 50x lens at a power of 10 % (5.05 mW). Raman spectra were obtained by accumulating 50
174 acquisitions of 10 s.

175

176 *2.4 Climatic monitoring*

177 The climatic conditions were monitored on the same step as the colorimetric measurements
178 (Supplementary fig. 1). The temperature inside the stone was monitored by drilling a hole in
179 the pink and white sections and installing a Telog R-3300 probe (Trimble Inc., Sunnyvale,
180 USA). This probe records temperatures between -20 and 60 °C with a resolution and an
181 accuracy of 0.01 °C. Environmental conditions were monitored by hanging a Telog R-2162
182 probe (Trimble Inc., Sunnyvale, USA) between the two areas to measure air temperature and
183 relative humidity. This probe records temperatures between -30 and 80 °C with a resolution of
184 0.12 °C and an accuracy of 0.4 %, and records relative humidity between 5 and 95 % with a
185 resolution of 0.1 % and an accuracy of 2 %. Each probe recorded a measurement once every
186 two hours. The environmental data collected in this study was then compared to reference
187 data for outdoor temperature and relative humidity were collected from a website
188 (www.historique-meteo.net).

189

190 *2.5 Microbiological analysis*

191 *2.5.1 Sampling*

192 Samples were taken from the white and pink areas of the same step for high-throughput
193 sequencing analysis of microbiological populations. Three samples were taken from the white
194 area (W1, W2 and W3) and from the pink area (P1, P2, P3). Samples were collected by
195 scratching a 25 cm² surface with a scalpel, providing a fine powder.

196

197 *2.5.2 Total genomic DNA extraction and high-throughput sequencing*

198 Bacterial, fungal and eukaryotic communities were identified for each sample. Total genomic
199 DNA was extracted from the samples and from an outgroup (O) composed of non-filtered
200 autoclaved water (“dead DNA” remained in the sample) using FastDNATM Spin Kit for soil
201 (MP Biomedicals, LLC, Santa Ana, USA), according to the manufacturer’s instructions.
202 High-throughput sequencing library preparation and Illumina Miseq (Illumina, San Diego,
203 USA) sequencing were conducted by Genoscreen (Lille, France). The Metabiote protocol
204 (Genoscreen, Lille, France) was used to prepare and barcode the twenty-one libraries (6
205 samples + 1 outgroup x 3 microbial communities), and targeted the 16S ribosomal V3 and V4
206 DNA hypervariable regions, the ITS1/ITS2 DNA region and the 18S ribosomal DNA region
207 for bacteria, fungi and eukaryotes, respectively. The twenty-seven libraries were then pooled
208 for single-run sequencing. Sequencing was performed with 4 pM of the pooled library using a
209 300-bp paired-end sequencing protocol on the Illumina MiSeq platform.

210

211 *2.5.3 Processing of high-throughput sequencing data*

212 The data were demultiplexed using CASAVA software (Illumina, San Diego, USA). After
213 primer removal, the sequences with a low Phred quality score (Q<30) were removed and the
214 overlapping paired-end reads were assembled using FLASH software (Magoč and Salzberg,
215 2011). Finally a QIIME 2 2018.11 pipeline was used to remove chimeric sequences, cluster
216 the sequences in operational taxonomic units (OTUs; quality-filter and deblur plugins; q-score
217 and denoise-16S/denoise-other functions) and taxonomically classify the obtained OTUs
218 (plugin feature-classifier; function classify-consensus-vsearch; (Bolyen et al., 2018)). The

219 taxonomic classification of bacterial, fungal and eukaryotic OTUs was achieved using
220 Greengenes database (McDonald et al., 2012), the UNITE database (Nilsson et al., 2018) and
221 the SILVA database (Quast et al., 2013), respectively.

222

223

224

225 2.6 Statistics

226 2.6.1 Colorimetric monitoring

227 Statistical analyses were carried out using R 3.2.5 with $\alpha = 5 \%$ (R Core Team, 2014). The
228 results of colorimetric measurements were analyzed by a generalized linear mixed model
229 (GLMM). The GLMM is a suitable analytical tool for non-normal data collected from
230 complicated designs involving random and fixed effects.

231 Four qualitative variables were used to design the GLMM, namely the *Color area* (two
232 modalities corresponding to the health status of the sampling area: *White* for the healthy part
233 of stones and *Pink* for the pink part of stones); *Covering* (two modalities: *Yes* for samples that
234 had been covered during the monitoring and *No* for all others); *Scratching* (two modalities:
235 *Yes* for samples which had been scratched prior to monitoring and *No* for all others); and
236 *Measurement date* (six modalities corresponding to the six measurement dates, i.e. *Sept. 2014*
237 *before scratching*, *Sept. 2014 after scratching*, *May 2015*, *Jan. 2016*, *July 2017*, and *Jan.*
238 *2018*).

239 The GLMM for this study was:

$$240 \text{Link}(p_{ijklm}) = \eta_{ijklm} = \theta + \alpha_i + \beta_j + \gamma_k + \delta_l + \alpha_i:\gamma_k + \alpha_i:\delta_l + \gamma_k:\delta_l + \alpha_i:\gamma_k:\delta_l + \mu_{ijkl} + \varepsilon_{ijklm}$$

241 where θ is the general effect, α_i is the effect of *Color area*, β_j is the effect of *Covering*, γ_k is
242 the effect of *Scratching*, δ_l is the effect of *Measurement date*, $\alpha_i:\gamma_k$ is the effect of the
243 interaction between *Color area* and *Scratching*, $\alpha_i:\delta_l$ is the effect of the interaction between
244 *Color area* and *Measurement date*, $\gamma_k:\delta_l$ is the effect of the interaction between *Scratching* and
245 *Measurement date*, $\alpha_i:\gamma_k:\delta_l$ is the effect of the triple interaction between *Color area*,
246 *Scratching* and *Measurement date*, μ_{ijkl} is the experimental error associated to each
247 measurement and ε_{ijklm} is the residual error. The effects of other interactions between variables
248 were not included in the model because they do not provide supplementary information. α , β ,
249 γ , δ , $\alpha:\gamma$, $\alpha:\delta$, $\gamma:\delta$ and $\alpha:\gamma:\delta$ were considered as fixed effects, while μ was considered as a
250 random effect. The term η_{ijklm} is known as the linear predictor. This term is obtained by
251 applying the variable p_{ijklm} to the link function of the model. The choice of the link function
252 depends on the p_{ijklm} distribution law. The identity link function is suitable for values provided
253 by colorimetric measurements, i.e. continuous data, either positive or negative (Wolfinger and
254 O'connell, 1993). GLMM parameters were estimated using the penalized quasi-likelihood
255 (PQL) technique (MASS package; glmmPQL function; Wolfinger and O'connell, 1993). A
256 Wald chi-square test was performed to determine the significance degree of each explanatory
257 variable in the GLMM (car package; Anova function; Fox, 2015). The GLMM was completed
258 with a Tukey's post-hoc test in order to check the significance of differences between means
259 (lsmeans package; lsmeans function; Bretz et al., 2016).

260

261 2.6.2 Climatic monitoring

262 The temperatures recorded in the white and pink areas of stone and in the air were compared
263 through a one-way analysis of variance (ANOVA; stats package; aov function; Fisher, 2006)
264 after checking the homogeneity of distribution variances with a Bartlett test (stats package;

265 bartlett.test function; Bartlett, 1937). This statistical test checks if the means of several
266 samples are equal, and is useful to compare three or more means. The ANOVA test was
267 completed by post-hoc analysis to rank the different means. The significance of differences
268 between means was assessed using Tukey's range test (multcomp package; glht function;
269 Faraway, 2002).

270 The relative air humidity values were used to calculate dew points to check for potential
271 condensation on the surface of the stone (weathermetrics package; function
272 humidity.to.dewpoint).

273 2.6.3 Alpha and beta diversity of microbial communities

274 Alpha diversity, i.e. the diversity of microbial species in each sample, and beta diversity, i.e.
275 the difference in microbial communities between samples, were identified using QIIME 2
276 2018.11. After generating a phylogenetic tree (phylogeny plugin; align-to-tree-mafft-fasttree
277 function), the Shannon's diversity index and the Pielou's evenness index were calculated to
278 characterize alpha diversity (diversity plugin; core-metrics-phylogenetic function; Hill, 1973),
279 while beta diversity was assessed through principle coordinates analysis (PCoA) based on the
280 determination of the Bray-Curtis distance (diversity plugin; core-metrics-phylogenetic
281 function; Legendre and Gallagher, 2001). The significance of the groups obtained was then
282 assessed with a Kruskal-Wallis non-parametric test for alpha diversity indexes (diversity
283 plugin; alpha-group-significance function; Hollander and Wolfe, 1999), and with
284 PERMANOVA for beta diversity (999 permutations; diversity plugin; beta-group-
285 significance function; Anderson, 2001).

286

287 3. Results

288

289 3.1 Colorimetric monitoring

290 Scratching the surface of the stone sufficed to completely remove any visible evidence of pink
291 coloration. The colors in both the white and pink areas showed no sign of change over the
292 three and a half years of monitoring: the scratched sections did not become pink again, and no
293 changes were observed in the colors of the white and pink areas on each of the two steps.

294 The results of the general linear mixed models designs were the same for the three dimensions
295 of the L*a*b* color space (Table 1): *Color area*, *Scratching* and *Measurement date* and
296 interactions between these factors all had a significant effect on the model, whereas *Covering*
297 did not. The effect of factors was more pronounced for L* and b* variables than for a*
298 variable. The measurements recorded in the unscratched pink area and the first measurement
299 made in September 2014 (i.e. before scratching) in the scratched pink area showed that the
300 pink area was characterized by a lower L* value and higher a* and b* values than those
301 recorded in the white area (Fig. 3 and supplementary fig. 2). The difference was statistically
302 supported for L* and b*, but not for a*. The difference recorded between sections that had not
303 been scratched remained the same throughout the study. Measurements recorded after
304 scratching in September 2014 showed that the scratching led to an increase in the L* value
305 and a decrease in a* and b* values in the pink and white areas. This difference in the
306 evolution of scratched areas was statistically supported by L* and b* values for the pink area
307 and only by the L* value for the white area. Finally, these differences remained statistically
308 stable in terms of L* and a* values for all studied modalities from after scratching in
309 September 2014 until the end of the colorimetric study in January 2018. The differences
310 remained statistically stable in terms of b* value from the second date of assessment, May
311 2015, until the end of the study. In other words, the significant effect of the *Date* factor was

312 almost entirely supported by the differences observed at the first date of assessment before
313 and after scratching and the color did not evolve until the end of the study, confirming visual
314 observations.

315

316 *3.2 Raman spectroscopy*

317 After baseline correction and removal of stone-related noise, Raman spectroscopy revealed
318 the presence of a pigment belonging to the family of carotenoids in the pink powder scratched
319 from the step (Supplementary fig. 3). Carotenoids are usually characterized by three peaks
320 corresponding to C–CH bending, C–C stretching and C=C stretching. C–C and C=C
321 stretching were clearly identifiable at 1151 and 1506 cm^{-1} , and C=CH₃ bending was also
322 present at 1003 cm^{-1} .

323

324 *3.3 Climatic monitoring*

325 The room temperature in the staircase ranged from 3.22 to 27.33 °C during the study (Table
326 2). Climatic monitoring showed that the room temperature was linked to the outside
327 temperature (Supplementary fig. 4a): the seasonal variations in temperature had a clear impact
328 on room air temperature, with low temperatures recorded during winter and warm
329 temperatures during summer. Daily room temperature variations due to day/night alternation
330 were less marked than those observed outdoors. Moreover, the room temperature was warmer
331 during winter and cooler during summer than the outside temperatures. The relative humidity
332 of room air ranged from 30.01 - 89.2 %. As observed for room temperature, variations in
333 relative humidity of room air followed those recorded for outside relative humidity, although
334 these values are lower than those recorded for outdoor relative humidity. Indoor relative
335 humidity remained between 45 and 65 % for most of the year and rarely exceeded 80 %
336 (Supplementary table 1).

337 The surface temperature in the white area and in the pink area followed room temperature
338 variations (Supplementary fig. 4b), but the temperature was significantly warmer in the pink
339 area than in both the white area and the room air (Supplementary table 2). The ANOVA study
340 also showed that the temperature in the white area was significantly lower than the room
341 temperature. However, this result should be considered with caution as the interval value was
342 lower than the accuracy of the ambient probe. Finally, the calculation of dew points from
343 ambient relative humidity and surface temperatures showed that no condensation could have
344 been formed at the surface of the step during the year of climatic monitoring.

345

346 *3.4 Alpha and beta diversity of microbial communities*

347 The only perceptible alpha diversity difference between the white and the pink areas was
348 related to bacterial communities (Supplementary table 3). Bacterial richness (Shannon index)
349 and equitability (Pielou's index) were higher in the pink area than in the white area, and this
350 difference is almost significantly supported (Supplementary table 4). No alpha diversity
351 difference was observed between sampling areas for fungal and eukaryote communities.

352 The study of beta diversity among bacterial communities clearly separated samples into two
353 groups on the first PCoA axis (Supplementary fig. 5): communities sampled in the pink area
354 shift to positive values on this axis as compared to communities sampled in the white area.
355 The community assessed in the outgroup sample was separated from the two other groups by
356 shifting to positive values on the second PCoA axis. The PERMANOVA test associated to the
357 study of beta diversity confirmed that the sampling area had a significant effect on bacterial

358 community composition, even if the post-hoc test failed to separate the white and pink areas
359 (Supplementary table 5). Conversely, the PCoA expressed no difference between sampling
360 areas in fungal and eukaryotes communities, with the communities of some samples located
361 closer to the outgroup sample than to other samples in the same area.

362 The assignment of OTUs revealed that the majority of the bacteria found in the white and in
363 the pink area were Actinobacteria, while the outgroup sample was dominated by
364 Proteobacteria. Among Actinobacteria, the communities of white area samples were largely
365 dominated by the genus *Rubrobacter*, while the communities of pink area samples were
366 largely dominated by the genus *Nitriliruptor* (Fig. 4). Low proportions of *Rubrobacter* were
367 also detected in pink area and low proportions of *Nitriliruptor* were also detected in white
368 area. All other bacterial taxa detected in white and pink areas were in low proportions.

369 The phylogenetic analysis of fungal and eukaryotes communities did not produce significant
370 differences between samples, especially regarding pink-pigmented yeasts or algae.

371

372 **4. Discussion**

373

374 *4.1 Bacterial origin of rosy discoloration*

375 The most important result of this study is the confirmation of the biological origin of the rosy
376 discoloration affecting the stone staircase in Sully-sur-Loire castle. Raman spectroscopy
377 assessment of the pink pigment produced on the stone revealed the characteristic bands of
378 C=C and C–C stretching and C–CH bending of carotenoids (De Oliveira et al., 2010). Next-
379 generation sequencing did not reveal any differences between fungal communities and more
380 generally between eukaryote communities on pink and white areas. Conversely, the
381 composition of bacterial communities was strongly related to the type of sampling area. This
382 result is in accordance with past studies that assigned such discoloration to bacterial biofilms
383 (Piñar et al., 2014a). Actinobacteria was the most abundant phylum identified in both pink
384 and white areas in our study. This phylum has already been widely reported in studies that
385 focused on the deterioration of stone in general (Gorbushina, 2007; McNamara and Mitchell,
386 2005; Zanardini et al., 2016), and on rosy discoloration in particular (Ettenuer et al., 2014;
387 Laiz et al., 2009; Tescari et al., 2018b). *Nitriliruptor* was the main bacterial genus identified
388 in the pink area, while *Rubrobacter* was the main genus identified in the white area. This
389 result differs from those obtained in past studies in which *Rubrobacter* was generally the main
390 genus associated with rosy discoloration (Jurado et al., 2012; Laiz et al., 2009; Nugari et al.,
391 2009). The unusual nature of this result led us to duplicate the study with new samples, but
392 the second batch of samples gave the same result (data not shown). *Nitriliruptor* is an
393 haloalkaliphilic actinobacterium first identified in soda lakes (Sorokin et al., 2009). This
394 single species genus has also been reported in saline-alkali soil (Peng et al., 2017) and in arid
395 soil (Neilson et al., 2012). The only reference of *Nitriliruptor* in the field of cultural heritage
396 was in mineral crystals found on the skin of an 18th century mummy (Kráková et al., 2018).
397 Consequently, this first evidence of the role played by *Nitriliruptor* in stone deterioration is of
398 interest. This bacterial genus has been poorly studied to date, but numerous highly similar
399 environmental clones of this genus have been identified, suggesting that this organism is quite
400 abundant in nature despite being rare in culture collections (Goodfellow et al., 2012a).

401

402 *4.2 Possible replacement of the main agent of rosy discoloration by Nitriliruptor sp.*

403 The main data about *Nitriliruptor* in relation with this study is that this species is not known
404 to produce pink pigment, with available strains described as colorless (Goodfellow et al.,
405 2012b). Moreover, the colorimetric assessment of the white and the pink areas showed no
406 evolution of the color in each area during the period of monitoring from the day the stone was
407 scratched in September 2014 and January 2018. The only significant change in color was
408 recorded at the beginning of the experiment between the measurements before scratching and
409 the measurements after scratching. This suggests that the process leading to the formation of
410 the rosy discoloration of stones was already finished at the beginning of the experiment and
411 that the presence of *Nitriliruptor* may indicate a subsequent evolution of this process.
412 Bacterioruberin-related carotenoids are frequently associated to *Rubrobacter sp.* and to the
413 rosy discoloration phenomenon on stones (Imperi et al., 2007). In our study, the position of
414 the bands in the Raman spectrum obtained from the pink powder corresponds to that expected
415 for bacterioruberin-related carotenoids (Jehlička et al., 2013; Marshall et al., 2007). A
416 plausible hypothesis is that the rosy discoloration may have been produced under the action of
417 *Rubrobacter* strains, which may have then been replaced by *Nitriliruptor* strains; the pigments
418 usually remain very stable on the materials, even if the causative microorganisms are already
419 dead (Piñar et al., 2014a). The development of pink biofilms on stone has often been linked to
420 water infiltrations and the formation of salt crystals (Piñar et al., 2014a). Carotenoids are
421 known to protect the cells against photo-oxidative damage and to act as membrane stabilizers
422 against salt stress (Köcher and Müller, 2011). The development of *Rubrobacter* would
423 therefore be favoured when desiccation occurs through temperature increase and salt
424 formation (Imperi et al., 2007; Laiz et al., 2009; Schabereiter-Gurtner et al., 2001).
425 Interestingly, the ecological niche of *Nitriliruptor* seems to be very close to that of
426 *Rubrobacter*; we have already mentioned that *Nitriliruptor* has been found in environments
427 with high salinity. The studies that highlighted the presence of *Nitriliruptor* strains in a habitat
428 also detected *Rubrobacter* strains (Ma and Gong, 2013; Neilson et al., 2012). The
429 *Nitriliruptor* development on the staircase of Sully-sur-Loire could therefore be a natural
430 progression of the *Rubrobacter* development under such environmental conditions. Further
431 studies about physicochemical properties of the stone should be performed to determine
432 whether particular conditions had favoured the development of *Nitriliruptor*. This is
433 particularly important in the light of this bacterial genus' ability to use short-chain organic
434 acids, amides and aliphatic nitriles as energy and carbon sources (Goodfellow et al., 2012b).
435 On the other hand, *Rubrobacter* was also detected on stones that did not suffer from rosy
436 discoloration (Chimienti et al., 2016; Li et al., 2016; Zanardini et al., 2019). It is not therefore
437 impossible that *Rubrobacter* DNA was detected in the white area of the staircase, especially
438 since the production of carotenoids by microorganism can vary largely according to
439 environmental conditions (Calegari-Santos et al., 2016; Fong et al., 2001).

440 The genus *Nitriliruptor* so far includes only one species (Sorokin et al., 2009). Considering
441 that the study of V3-V4 16s rRNA region is not accurate enough to provide species definition
442 (Bukin et al., 2019), and that Actinobacteria are frequently carotenoid producers (Klassen,
443 2010), the possibility that *Nitriliruptor sp.* detected on the staircase is a new undescribed
444 carotenoid producer species cannot either be dismissed. The production of carotenoid by this
445 species could also vary largely according to environmental conditions. A shotgun
446 metagenomics approach would help to answer this question in future studies by reconstructing
447 the partial genome of the most prevalent species in the samples thus testing the presence of
448 carotenoid synthesis genes.

449

450 *4.3 Environmental factors involved in the development of rosy discoloration*

451 Previous studies have noted that the development of pink biofilms has often been linked to
452 problems of water infiltration and salt crystallization, and in some cases could be associated
453 with the combined effect of an increase in temperature and the sudden decrease in water
454 availability when the infiltration problem is solved (Imperi et al., 2007; Laiz et al., 2009). The
455 climatic monitoring of the staircase showed that no condensation theoretically occurred at the
456 surface of the stone during the year of study: indeed, the temperature recorded at this surface
457 stayed above the dew point. Moreover, the relative humidity in the staircase air appeared
458 relatively adequate in terms of conservation conditions. It released between 45 and 65 % of
459 humidity more than 60 % of the time, which corresponds to the relative humidity values
460 generally advised for conservation (D'Agostino et al., 2014; Merello et al., 2012).
461 Nevertheless, this humidity range could be problematic if nitrates are present: sodium nitrate
462 and magnesium nitrate crystallize when relative humidity drops below 60 % (Arnold and
463 Zehnder, 1991). However, no efflorescence had been noted in the staircase during the
464 observations and the presence of soluble salts was not assessed during this study. The origin
465 of the water and of possible salt crystallization is most likely the result of external rainfall
466 seeping through the external wall of the staircase. The location of the biofilm at the surface of
467 the staircase steps supports this hypothesis: only the external part of the steps is affected, and
468 the upper part of the staircase seemed to be more affected than the lower part. The
469 administrators of the castle confirmed that external infiltration occurred through the roof of
470 the stairwell, and that the problem had since been resolved. This reinforces the hypothesis that
471 the rosy discoloration observed at the stone surface of the staircase corresponds to a past
472 phenomenon which no longer occurs. Finally, the climatic monitoring showed that the
473 temperature at the stone surface in the pink area was slightly higher than the temperature in
474 the white area. This could have emphasized the desiccation phenomenon and favoured the
475 development of *Rubrobacter* in the pink area (Imperi et al., 2007; Schabereiter-Gurtner et al.,
476 2001).

477 These observations may explain the distribution of the pink area on the staircase surface and
478 could indicate the action of several factors: the infiltration of external water through the wall,
479 the subsequent formation of salts through crystallization and dissolution process, and the
480 microclimatic differences of temperature occurring at the surface of the staircase.

481

482 **5. Conclusions**

483

484 The study confirms that the rosy discoloration occurring at the surface of the spiral staircase
485 was due to bacterial growth. Bacteria belonging to *Rubrobacter* genus may have been the
486 main producer of pink pigment, before being replaced by bacteria from the *Nitriiliruptor*
487 genus. Further studies about the physicochemical properties of the stone should be performed
488 to determine if specific conditions favored the development of *Nitriiliruptor*.

489

490 **Acknowledgment**

491

492 We thank Joanna Lignot for English language editing.

493 **References**

494

495 Abadía, O.M., Morales, M.R.G., 2013. Paleolithic art: a cultural history. *J. Archeol. Res.* 21,
496 269-306, <https://dx.doi.org/10.1007/s10814-012-9063-8>.

497 Anderson, M.J., 2001. A new method for non-parametric multivariate analysis of variance.
498 *Austral Ecol.* 26, 32-46, <https://dx.doi.org/doi:10.1111/j.1442-9993.2001.01070.pp.x>.

499 Arnold, A., Zehnder, K., 1991. Monitoring wall paintings affected by soluble salts, In: Cather,
500 S. (Ed.), *The conservation of wall paintings*. Oxford University Press, Oxford, pp.
501 103-135.

502 Bartlett, M.S., 1937. Properties of sufficiency and statistical tests. *Proc. R. Soc. Lond. A* 160,
503 268-282, <https://dx.doi.org/10.1098/rspa.1937.0109>.

504 Berdoulay, M., Salvado, J., 2009. Genetic characterization of microbial communities living at
505 the surface of building stones. *Lett. Appl. Microbiol.* 49, 311-316,
506 <https://dx.doi.org/10.1111/j.1472-765X.2009.02660.x>.

507 Bolyen, E., Rideout, J.R., Dillon, M.R., Bokulich, N.A., Abnet, C., Al-Ghalith, G.A.,
508 Alexander, H., Alm, E.J., Arumugam, M., Asnicar, F., 2018. QIIME 2: Reproducible,
509 interactive, scalable, and extensible microbiome data science. *PeerJ PrePrints*,
510 <https://dx.doi.org/10.7287/peerj.preprints.27295v2>.

511 Bretz, F., Hothorn, T., Westfall, P., 2016. *Multiple comparisons using R*. CRC Press, Boca
512 Raton.

513 Brimblecombe, P., Grossi, C.M., 2009. Millennium-long damage to building materials in
514 London. *Sci. Total Environ.* 407, 1354-1361,
515 <https://dx.doi.org/10.1016/j.scitotenv.2008.09.037>.

516 Bukin, Yu.S., Galachyants, Yu.P., Morozov, I.V., Bukin, S.V., Zakharenko, A.S., Zemskeya,
517 T.I., 2019. The effect of 16S rRNA region choice on bacterial community
518 metabarcoding results. *Sci. Data.* 6, <https://dx.doi.org/10.1038/sdata.2019.7>.

519 Calegari-Santos, R., Diogo, R.A., Fontana, J.D., Bonfim, T.M.B., 2016. Carotenoid
520 production by halophilic archaea under different culture conditions. *Curr. Microbiol.*
521 72, 641-651, <https://dx.doi.org/10.1007/s00284-015-0974-8>.

522 Caneva, G., Gori, E., Montefinale, T., 1995. Biodeterioration of monuments in relation to
523 climatic changes in Rome between 19–20th centuries. *Sci. Total Environ.* 167, 205-
524 214, [https://dx.doi.org/10.1016/0048-9697\(95\)04581-K](https://dx.doi.org/10.1016/0048-9697(95)04581-K).

525 Chimienti, G., Piredda, R., Pepe, G., van der Werf, I.D., Sabbatini, L., Crecchio, C., Ricciuti,
526 P., D’Erchia, A.M., Manzari, C., Pesole, G., 2016. Profile of microbial communities
527 on carbonate stones of the medieval church of San Leonardo di Siponto (Italy) by
528 Illumina-based deep sequencing. *Appl. Microbiol. Biot.* 100, 8537-8548,
529 <https://dx.doi.org/10.1007/s00253-016-7656-8>.

530 Crispim, C., Gaylarde, C., 2005. Cyanobacteria and biodeterioration of cultural heritage: a
531 review. *Microb. Ecol.* 49, 1-9, <https://dx.doi.org/10.1007/s00248-003-1052-5>.

532 D’Agostino, D., Congedo, P.M., Cataldo, R., 2014. Computational fluid dynamics (CFD)
533 modeling of microclimate for salts crystallization control and artworks conservation. *J.*
534 *Cult. Herit.* 15, 448-457,
535 <https://dx.doi.org/https://doi.org/10.1016/j.culher.2013.10.002>.

- 536 De Felice, B., Pasquale, V., Tancredi, N., Scherillo, S., Guida, M., 2010. Genetic fingerprint
537 of microorganisms associated with the deterioration of an historical tuff monument in
538 Italy. *J. Genet.* 89, 253-257, <https://dx.doi.org/10.1007/s12041-010-0035-9>.
- 539 De Oliveira, V.E., Castro, H.V., Edwards, H.G., De Oliveira, L.F.C., 2010. Carotenes and
540 carotenoids in natural biological samples: a Raman spectroscopic analysis. *J. Raman.*
541 *Spectrosc.* 41, 642-650, <https://dx.doi.org/10.1002/jrs.2493>.
- 542 Ettenauer, J.D., Jurado, V., Piñar, G., Miller, A.Z., Santner, M., Saiz-Jimenez, C., Sterflinger,
543 K., 2014. Halophilic microorganisms are responsible for the rosy discolouration of
544 saline environments in three historical buildings with mural paintings. *PLoS One* 9,
545 0103844, <https://dx.doi.org/10.1371/journal.pone.0103844>.
- 546 Faraway, J.J., 2002. *Practical regression and ANOVA using R*. University of Bath, Bath.
- 547 Fisher, R.A., 2006. *Statistical methods for research workers*. Genesis Publishing Pvt Ltd,
548 Guildford.
- 549 Fong, N.I., Burgess, M., Barrow, K., Glenn, D., 2001. Carotenoid accumulation in the
550 psychrotrophic bacterium *Arthrobacter agilis* in response to thermal and salt stress.
551 *Appl. Microbiol. Biot.* 56, 750-756, <https://dx.doi.org/10.1007/s002530100739>.
- 552 Fox, J., 2015. *Applied regression analysis and generalized linear models*. Sage Publications,
553 Thousand Oaks.
- 554 Goodfellow, M., Kämpfer, P., Busse, H.-J., Trujillo, M.E., Suzuki, K.-i., Ludwig, W.,
555 Whitman, W.B., 2012a. *Bergey's manual® of systematic bacteriology: volume five*
556 *the actinobacteria, part A*. Springer, New York.
- 557 Goodfellow, M., Kämpfer, P., Busse, H.-J., Trujillo, M.E., Suzuki, K.-i., Ludwig, W.,
558 Whitman, W.B., 2012b. *Bergey's manual® of systematic bacteriology: volume five*
559 *the actinobacteria, part B*. Springer, New York.
- 560 Gorbushina, A.A., 2007. Life on the rocks. *Environ. Microbiol.* 9, 1613-1631,
561 <https://dx.doi.org/10.1111/j.1462-2920.2007.01301.x>.
- 562 Gorbushina, A.A., Andreas, B., Schulte, A., 2005. Microcolonial rock inhabiting fungi and
563 lichen photobionts: evidence for mutualistic interactions. *Mycol. Res.* 109, 1288-1296,
564 <https://dx.doi.org/10.1017/S0953756205003631>.
- 565 Guillitte, O., 1995. Bioreceptivity: a new concept for building ecology studies. *Sci. Total*
566 *Environ.* 167, 215-220, [https://dx.doi.org/10.1016/0048-9697\(95\)04582-L](https://dx.doi.org/10.1016/0048-9697(95)04582-L).
- 567 Gurtner, C., Heyrman, J., Piñar, G., Lubitz, W., Swings, J., Rölleke, S., 2000. Comparative
568 analyses of the bacterial diversity on two different biodeteriorated wall paintings by
569 DGGE and 16S rDNA sequence analysis. *Int. Biodeter. Biodegr.* 46, 229-239,
570 [https://dx.doi.org/10.1016/S0964-8305\(00\)00079-2](https://dx.doi.org/10.1016/S0964-8305(00)00079-2).
- 571 Hill, M.O., 1973. Diversity and evenness: a unifying notation and its consequences. *Ecology*,
572 427-432, <https://dx.doi.org/10.2307/1934352>.
- 573 Hollander, M., Wolfe, D.A., 1999. *Nonparametric statistical methods*. Wiley, Chichester.
- 574 Hoppert, M., König, S., 2006. The succession of biofilms on building stone and its possible
575 impact on biogenic weathering, In: Fort, R., Alvarez de Buergo, M., Gomez-Heras,
576 M., Vazquez-Ciervo, C. (Eds.), *Heritage, weathering and conservation*. Taylor and
577 Francis Group, London, pp. 311-315.
- 578 Hueck, H., 1965. The biodeterioration of materials as a part of hylobiology. *Mater.*
579 *Organismen* 1, 5-34.

- 580 Imperi, F., Caneva, G., Cancellieri, L., Ricci, M.A., Sodo, A., Visca, P., 2007. The bacterial
581 aetiology of rosy discoloration of ancient wall paintings. *Environ. Microbiol.* 9, 2894-
582 2902, <https://dx.doi.org/10.1111/j.1462-2920.2007.01393.x>.
- 583 Janvier-Badosa, S., Beck, K., Brunetaud, X., Guirimand-Dufour, A., Al-Mukhtar, M., 2015.
584 Gypsum and spalling decay mechanism of tuffeau limestone. *Environ. Earth Sci.* 74,
585 2209-2221, <https://dx.doi.org/10.1007/s12665-015-4212-2>.
- 586 Jehlička, J., Edwards, H.G.M., Oren, A., 2013. Bacterioruberin and salinixanthin carotenoids
587 of extremely halophilic Archaea and Bacteria: A Raman spectroscopic study.
588 *Spectrochim. Acta A* 106, 99-103,
589 <https://dx.doi.org/https://doi.org/10.1016/j.saa.2012.12.081>.
- 590 Jurado, V., Miller, A.Z., Alias-Villegas, C., Laiz, L., Saiz-Jimenez, C., 2012. *Rubrobacter*
591 *bracarensis* sp. nov., a novel member of the genus *Rubrobacter* isolated from a
592 biodeteriorated monument. *Syst. Appl. Microbiol.* 35, 306-309,
593 <https://dx.doi.org/10.1016/j.syapm.2012.04.007>.
- 594 Klassen, J.L., 2010. Phylogenetic and evolutionary patterns in microbial carotenoid
595 biosynthesis are revealed by comparative genomics. *PLoS One* 5, 11257,
596 <https://dx.doi.org/10.1371/journal.pone.0011257>.
- 597 Köcher, S., Müller, V., 2011. The nature and function of carotenoids in the moderately
598 halophilic bacterium *Halobacillus halophilus*, In: Ventosa, A., Oren, A., Ma, Y. (Eds.),
599 *Halophiles and Hypersaline Environments*. Springer, New York, pp. 303-317.
- 600 Korkanç, M., Savran, A., 2015. Impact of the surface roughness of stones used in historical
601 buildings on biodeterioration. *Constr. Build Mater.* 80, 279-294,
602 <https://dx.doi.org/10.1016/j.conbuildmat.2015.01.073>.
- 603 Kraková, L., Šoltys, K., Puškárová, A., Bučková, M., Jeszeová, L., Kucharík, M., Budiš, J.,
604 Orovčík, L.u., Szemes, T., Pangallo, D., 2018. The microbiomes of a XVIII century
605 mummy from the castle of Krásna Hôrka (Slovakia) and its surrounding environment.
606 *Environ. Microbiol.* 20, 3294-3308, <https://dx.doi.org/10.1111/1462-2920.14312>.
- 607 Laiz, L., Miller, A.Z., Jurado, V., Akatova, E., Sanchez-Moral, S., Gonzalez, J.M., Dionísio,
608 A., Macedo, M.F., Saiz-Jimenez, C., 2009. Isolation of five *Rubrobacter* strains from
609 biodeteriorated monuments. *Naturwissenschaften* 96, 71-79,
610 <https://dx.doi.org/10.1007/s00114-008-0452-2>.
- 611 Legendre, P., Gallagher, E.D., 2001. Ecologically meaningful transformations for ordination
612 of species data. *Oecologia* 129, 271-280, <https://dx.doi.org/10.1007/s004420100716>.
- 613 Li, Q., Zhang, B., He, Z., Yang, X., 2016. Distribution and diversity of bacteria and fungi
614 colonization in stone monuments analyzed by high-throughput sequencing. *PLoS One*
615 11, 0163287, <https://dx.doi.org/10.1371/journal.pone.0163287>.
- 616 Lisci, M., Monte, M., Pacini, E., 2003. Lichens and higher plants on stone: a review. *Int.*
617 *Biodeter. Biodegr.* 51, 1-17, [https://dx.doi.org/10.1016/S0964-8305\(02\)00071-9](https://dx.doi.org/10.1016/S0964-8305(02)00071-9).
- 618 Ma, B., Gong, J., 2013. A meta-analysis of the publicly available bacterial and archaeal
619 sequence diversity in saline soils. *World J. Microb. Biot.* 29, 2325-2334,
620 <https://dx.doi.org/10.1007/s11274-013-1399-9>
- 621 Macedo, M.F., Miller, A.Z., Dionísio, A., Saiz-Jimenez, C., 2009. Biodiversity of
622 cyanobacteria and green algae on monuments in the Mediterranean Basin: an
623 overview. *Microbiology* 155, 3476-3490, <https://dx.doi.org/10.1099/mic.0.032508-0>.

- 624 Magoč, T., Salzberg, S.L., 2011. FLASH: fast length adjustment of short reads to improve
625 genome assemblies. *Bioinformatics* 27, 2957-2963,
626 <https://dx.doi.org/10.1093/bioinformatics/btr507>.
- 627 Marshall, C.P., Leuko, S., Coyle, C.M., Walter, M.R., Burns, B.P., Neilan, B.A., 2007.
628 Carotenoid analysis of halophilic archaea by resonance Raman spectroscopy.
629 *Astrobiology* 7, 631-643, <https://dx.doi.org/10.1089/ast.2006.0097>.
- 630 McDonald, D., Price, M.N., Goodrich, J., Nawrocki, E.P., DeSantis, T.Z., Probst, A.,
631 Andersen, G.L., Knight, R., Hugenholtz, P., 2012. An improved Greengenes
632 taxonomy with explicit ranks for ecological and evolutionary analyses of bacteria and
633 archaea. *ISME J.* 6, 610, <https://dx.doi.org/10.1038/ismej.2011.139>.
- 634 McNamara, C.J., Mitchell, R., 2005. Microbial deterioration of historic stone. *Front. Ecol.*
635 *Environ.* 3, 445-451, [https://dx.doi.org/10.1890/1540-9295\(2005\)003\[0445:MDOHS\]2.0.CO;2](https://dx.doi.org/10.1890/1540-9295(2005)003[0445:MDOHS]2.0.CO;2).
- 637 Merello, P., García-Diego, F.-J., Zarzo, M., 2012. Microclimate monitoring of Ariadne's
638 house (Pompeii, Italy) for preventive conservation of fresco paintings. *Chem. Cent. J.*
639 6, 145, <https://dx.doi.org/10.1186/1752-153X-6-145>.
- 640 Miller, A.Z., Sanmartín, P., Pereira-Pardo, L., Dionísio, A., Saiz-Jimenez, C., Macedo, M.F.,
641 Prieto, B., 2012. Bioreceptivity of building stones: A review. *Sci. Total Environ.* 426,
642 1-12, <https://dx.doi.org/10.1016/j.scitotenv.2012.03.026>.
- 643 Neilson, J.W., Quade, J., Ortiz, M., Nelson, W.M., Legatzki, A., Tian, F., LaComb, M.,
644 Betancourt, J.L., Wing, R.A., Soderlund, C.A., 2012. Life at the hyperarid margin:
645 novel bacterial diversity in arid soils of the Atacama Desert, Chile. *Extremophiles* 16,
646 553-566, <https://dx.doi.org/10.1007/s00792-012-0454-z>.
- 647 Nilsson, R.H., Larsson, K.-H., Taylor, A.F.S., Bengtsson-Palme, J., Jeppesen, T.S., Schigel,
648 D., Kennedy, P., Picard, K., Glöckner, F.O., Tedersoo, L., Saar, I., Kõljalg, U.,
649 Abarenkov, K., 2018. The UNITE database for molecular identification of fungi:
650 handling dark taxa and parallel taxonomic classifications. *Nucleic Acids Res.* 47,
651 D259-D264, <https://dx.doi.org/10.1093/nar/gky1022>.
- 652 Nugari, M.P., Pietrini, A.M., Caneva, G., Imperi, F., Visca, P., 2009. Biodeterioration of
653 mural paintings in a rocky habitat: The Crypt of the Original Sin (Matera, Italy). *Int.*
654 *Biodeter. Biodegr.* 63, 705-711, <https://dx.doi.org/10.1016/j.ibiod.2009.03.013>.
- 655 Peng, M., Jia, H., Wang, Q., 2017. The effect of land use on bacterial communities in saline-
656 alkali soil. *Curr. Microbiol.* 74, 325-333, <https://dx.doi.org/10.1007/s00284-017-1195-0>.
- 658 Piñar, G., Ettenauer, J., Sterflinger, K., 2014a. La vie en rose': a review of rosy discoloration
659 of subsurface monuments, In: Saiz-Jimenez, C. (Ed.), *The conservation of*
660 *subterranean cultural heritage*. CRC Press, Boca Raton, pp. 113-123.
- 661 Piñar, G., Kraková, L., Pangallo, D., Piombino-Mascoli, D., Maixner, F., Zink, A., Sterflinger,
662 K., 2014b. Halophilic bacteria are colonizing the exhibition areas of the Capuchin
663 Catacombs in Palermo, Italy. *Extremophiles* 18, 677-691,
664 <https://dx.doi.org/10.1007/s00792-014-0649-6>.
- 665 Pinheiro, A.C., Mesquita, N., Trovão, J., Soares, F., Tiago, I., Coelho, C., de Carvalho, H.P.,
666 Gil, F., Catarino, L., Piñar, G., Portugal, A., 2018. Limestone biodeterioration: A
667 review on the Portuguese cultural heritage scenario. *J. Cult. Herit.*,
668 <https://dx.doi.org/10.1016/j.culher.2018.07.008>.

669 Quast, C., Pruesse, E., Yilmaz, P., Gerken, J., Schweer, T., Yarza, P., Peplies, J., Glöckner,
670 F.O., 2013. The SILVA ribosomal RNA gene database project: improved data
671 processing and web-based tools. *Nucleic Acids Res.* 41, D590-D596,
672 <https://dx.doi.org/10.1093/nar/gks1219>.

673 R Core Team, 2014. R: A language and environment for statistical computing. Vienna,
674 Austria: R Foundation for Statistical Computing; 2014.

675 Salvadori, O., Municchia, A.C., 2016. The role of fungi and lichens in the biodeterioration of
676 stone monuments. *Open Conf. Proc. J.* 7,
677 <https://dx.doi.org/10.2174/2210289201607020039>.

678 Schabereiter-Gurtner, C., Piñar, G., Vybiral, D., Lubitz, W., Rölleke, S., 2001. *Rubroacter*-
679 related bacteria associated with rosy discolouration of masonry and lime wall
680 paintings. *Arch. Microbiol.* 176, 347-354, <https://dx.doi.org/10.1007/s002030100333>.

681 Scheerer, S., Ortega-Morales, O., Gaylarde, C., 2009. Microbial deterioration of stone
682 monuments—an updated overview. *Adv. Appl. Microbiol.* 66, 97-139,
683 [https://dx.doi.org/10.1016/S0065-2164\(08\)00805-8](https://dx.doi.org/10.1016/S0065-2164(08)00805-8).

684 Sorokin, D.Y., van Pelt, S., Tourova, T.P., Evtushenko, L.I., 2009. *Nitriliruptor alkaliphilus*
685 gen. nov., sp. nov., a deep-lineage haloalkaliphilic actinobacterium from soda lakes
686 capable of growth on aliphatic nitriles, and proposal of Nitriliruptoraceae fam. nov.
687 and Nitriliruptorales ord. nov. *Int. J. Syst. Evol. Micr.* 59, 248-253,
688 <https://dx.doi.org/10.1099/ijs.0.002204-0>.

689 Sterflinger, K., Piñar, G., 2013. Microbial deterioration of cultural heritage and works of art -
690 tilting at windmills? *Appl. Microbiol. Biot.* 97, 9637-9646,
691 <https://dx.doi.org/10.1007/s00253-013-5283-1>.

692 Tescari, M., Frangipani, E., Caneva, G., Casanova Municchia, A., Sodo, A., Visca, P., 2018a.
693 *Arthrobacter agilis* and rosy discoloration in “Terme del Foro” (Pompeii, Italy). *Int.*
694 *Biodeter. Biodegr.*, <https://dx.doi.org/10.1016/j.ibiod.2018.03.015>.

695 Tescari, M., Visca, P., Frangipani, E., Bartoli, F., Rainer, L., Caneva, G., 2018b. Celebrating
696 centuries: Pink-pigmented bacteria from rosy patinas in the House of Bicentenary
697 (Herculaneum, Italy). *J. Cult. Herit.*, <https://dx.doi.org/10.1016/j.culher.2018.02.015>.

698 Thornbush, M., Viles, H., 2006. Changing patterns of soiling and microbial growth on
699 building stone in Oxford, England after implementation of a major traffic scheme. *Sci.*
700 *Total. Environ.* 367, 203-211, <https://dx.doi.org/10.1016/j.scitotenv.2005.11.022>.

701 Warscheid, T., Braams, J., 2000. Biodeterioration of stone: a review. *Int. Biodeter. Biodegr.*
702 46, 343-368, [https://dx.doi.org/10.1016/S0964-8305\(00\)00109-8](https://dx.doi.org/10.1016/S0964-8305(00)00109-8).

703 Wolfinger, R., O'connell, M., 1993. Generalized linear mixed models a pseudo-likelihood
704 approach. *J. Stat. Comput. Sim.* 48, 233-243,
705 <https://dx.doi.org/10.1080/00949659308811554>.

706 Zanardini, E., May, E., Inkpen, R., Cappitelli, F., Murrell, J.C., Purdy, K.J., 2016. Diversity
707 of archaeal and bacterial communities on exfoliated sandstone from Portchester Castle
708 (UK). *Int. Biodeter. Biodegr.* 109, 78-87,
709 <https://dx.doi.org/10.1016/j.ibiod.2015.12.021>.

710 Zanardini, E., May, E., Purdy, K.J., Murrell, J.C., 2019. Nutrient cycling potential within
711 microbial communities on culturally important stoneworks. *Env. Microbiol. Rep.* 11,
712 147-154, <https://dx.doi.org/10.1111/1758-2229.12707>.

713

714 Table 1: Effect of the qualitative variables on L*a*b* color space values, assessed with a
 715 Wald X^2 test associated with GLMMs.

<i>Source of variation</i>	<i>L</i>		<i>a</i>		<i>b</i>	
	X^2 -value	p-value	X^2 -value	p-value	X^2 -value	p-value
<i>Color area (Co)</i>	802	<0.001***	71	<0.001***	366	<0.001***
<i>Covering (C)</i>	1.2	0.26	2.1	0.15	0.2	0.65
<i>Scratching (S)</i>	1052	<0.001***	44	<0.001***	768	<0.001***
<i>Date (D)</i>	1062	<0.001***	57	<0.001***	1163	<0.001***
<i>Co:S</i>	255	<0.001***	19	<0.001***	291	<0.001***
<i>Co:D</i>	27	<0.001***	22	<0.001***	78	<0.001***
<i>S:D</i>	423	<0.001***	21	<0.001***	264	<0.001***
<i>Co:S:D</i>	74	<0.001***	13	0.02*	74	<0.001***

716 * p < 0.05, ** p < 0.01, *** p < 0.001

717

718 Table 2: Summary of climatic data assessed on the stone steps between September 2014 and
 719 January 2018.

<i>Color area</i>	<i>Temperature (°C)</i>			<i>Relative humidity (%)</i>		
	<i>Minimum</i>	<i>Mean</i>	<i>Maximum</i>	<i>Minimum</i>	<i>Mean</i>	<i>Maximum</i>
White	3.22	14.35	25.78	(-)	(-)	(-)
Pink	4.44	15.39	26.67	(-)	(-)	(-)
Room air	3.22	14.66	27.33	30.01	58.95	89.2
Outdoor	-3	12.53	35	43	80.65	98

720 (-): parameter not assessed

721

722 **Captions for Figures**

723 Figure 1: Location of the study area in Sully-sur-Loire castle.

724 The study focused on the stones of the “escalier d’honneur” of the donjon (a). The cross-
725 section of the “escalier d’honneur” shows the location of the pink discoloration (b).

726 3D model realized with SketchUp 2016 from plans, video recordings and pictures.

727

728 Figure 2: Half-pink step chosen for colorimetric and climatic monitoring.

729 The picture shows the distribution of the rosy discoloration on the outer part of the stairs.

730

731 Figure 3: 3D representation of the colorimetric monitoring of the stone step in the L*a*b*
732 colour space.

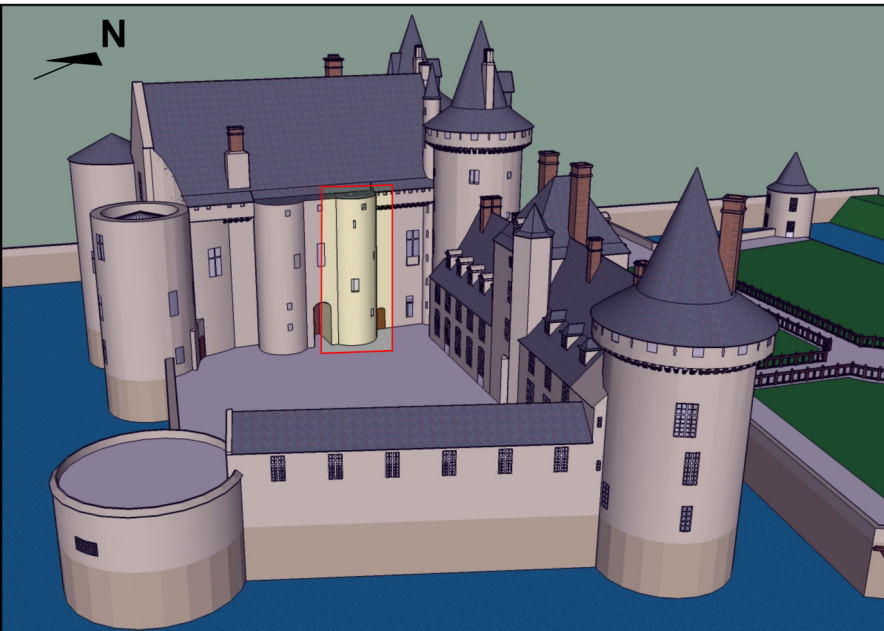
733 Values are depicted for the pink and in the white areas, scratched (crosses) or not (circles),
734 between September 2014 and January 2018.

735

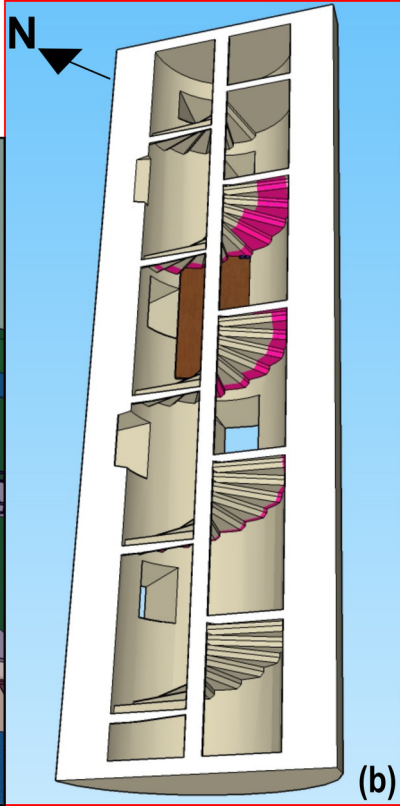
736 Figure 4: Heatmap of bacterial communities according to each sample at the genus level.

737 W: white sample; P: pink sample; O: outgroup sample.

738 The most abundant genera are labelled in pale blue, while the less abundant genera are
739 labelled in dark blue. The dendrograms show the proximity between the different samples and
740 the proximity between identified bacterial genera.

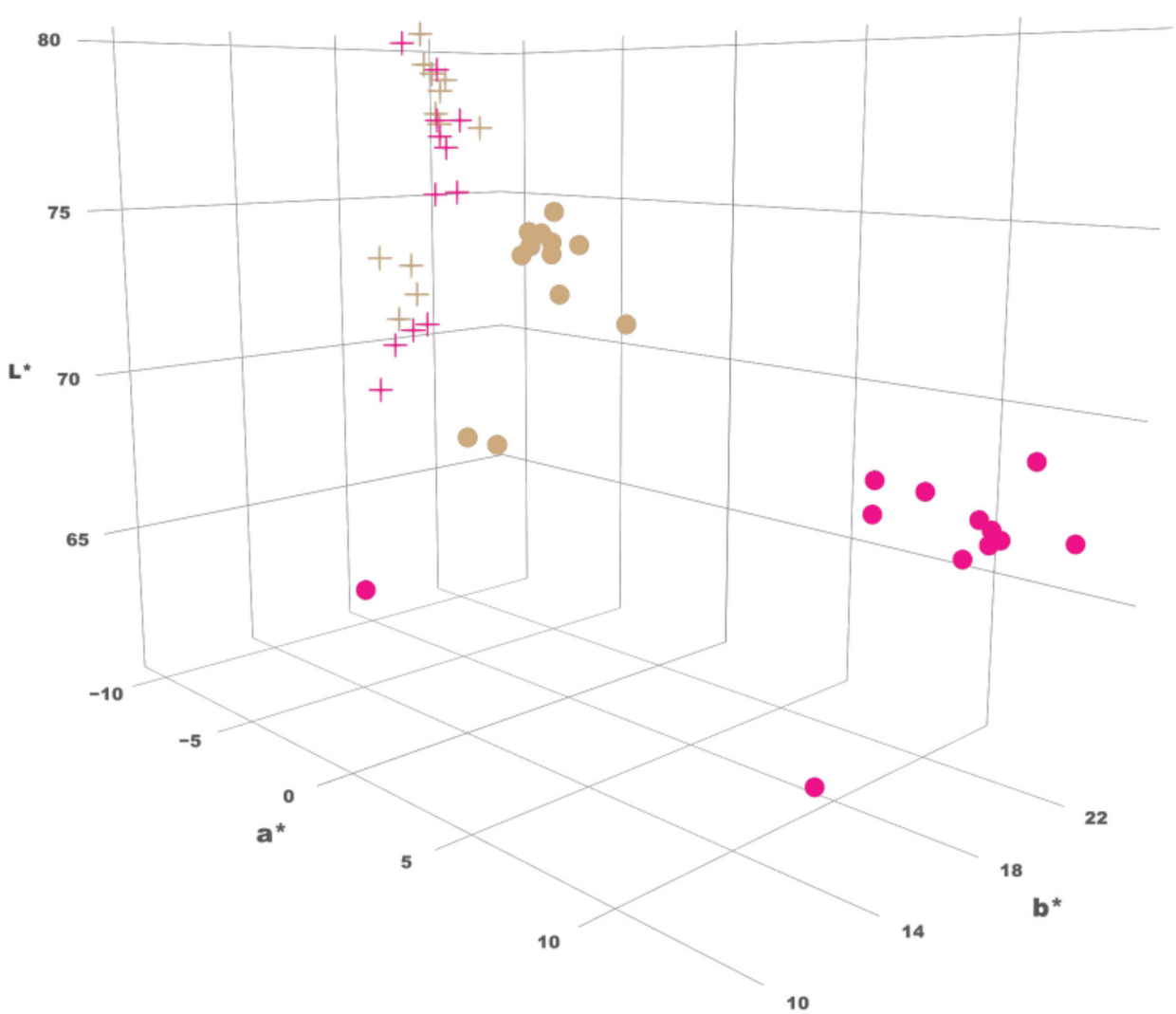


(a)



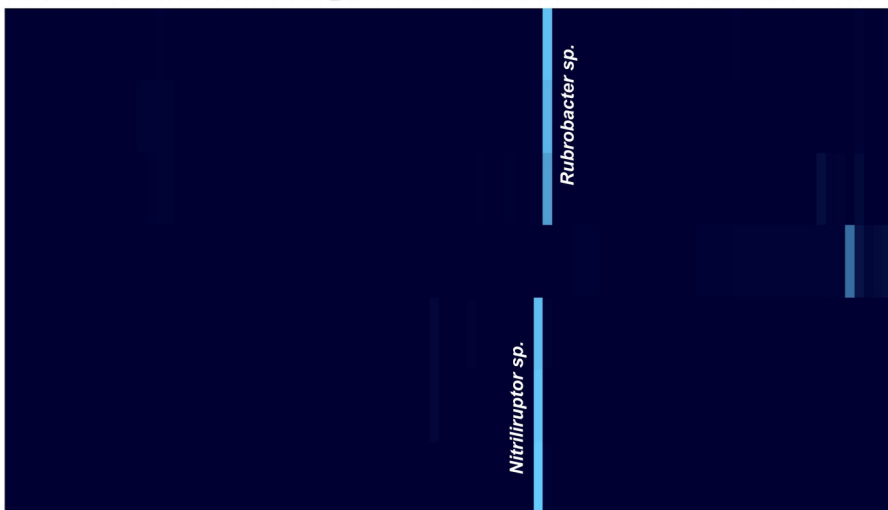
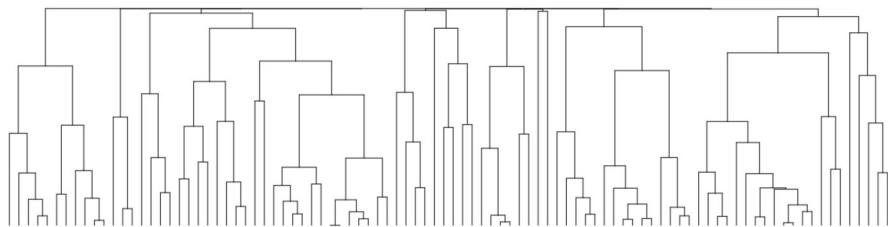
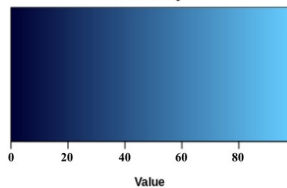
(b)





- Pink zone / Not scratched
- ✦ Pink zone / Scratched
- White zone / Not scratched
- ✦ White zone / Scratched

Color Key



W2
W1
W3
O
P3
P2
P1

Samples

Achromobacter
g__Psychrobacter
NA
g__Lamia
NA
g__Lysobacter
g__Chelatococcus
NA
NA
g__Litorilinea
NA
g__Aerifactor
g__Salinisphaera
Bacillus
g__Halomonas
g__Sakagamiibacter
NA
g__Nocardia
g__Burkholderia
NA
NA
g__Deftia
g__Mucobacterium
g__Rhizobium
NA
NA
g__Tolypotrux
g__Wersella
NA
g__Beutenbergia
g__Thermanaerofrix
g__Halobacterium
g__Mucosus
g__Spirosoma
NA
NA
g__Eluzobium
NA
g__Brevibacterium
g__Herbaspirillum
g__Helicobacillus
g__Acidovorax
g__Sphingomonas
g__Nitriliruptor
g__Paenibacillus
g__R__g__Dierzia
Methylobacterium
g__Azobacterium
NA
g__Staphylococcus
g__Pseudomonas
g__Prevotellia
g__Luminoibacter
g__Aurantimonas
NA
NA
g__Achetobacter
g__Corynebacterium
NA
NA
g__Achromobacter
g__Rickettsia
NA
g__Tetradiphthia
g__Lactobacillus
g__Propionibacterium
g__Streptococcus
NA
g__Pseudomonas
NA
g__Escherichia
g__Pseudoxanthomonas
NA
NA

Taxonomy

Nitriliruptor sp.* *Rubrobacter sp.

W1	0.7 %	86.5 %
W2	0.00 %	92.8 %
W3	0.3 %	76.8 %
P1	97.7 %	0.6 %
P2	95 %	0.5 %
P3	91.8 %	1.00 %
O	0.00 %	0.00 %